Electronic Supplementary Material (ESI) for Physical Chemistry Chemical Physics.

Electronic Supplementary Information for "Anomalously Supercooled H_2-D_2 Mixtures Flowing inside a Carbon Nano Tube"

I-Ya Chang, Shutaro Yamaoka, and Kim Hyeon-Deuk*

Department of Chemistry, Kyoto University, Kyoto, 606-8502, Japan

E-mail: kim@kuchem.kyoto-u.ac.jp,Phone:+81-75-753-4021

*To whom correspondence should be addressed

S1: COMPUTATIONAL DETAILS

All the density functional theory (DFT) calculations were done with the PBE functional and PAW pseudopotentials implemented in the VASP package.[1] The length of the periodic unit cell is 8.52 Å along the CNT(15,0) axis (z-axis) while the vacuum of approximately 1 nm and 2 nm was inserted into the x- and y-directions, respectively. The energy cutoff for the plane wave basis is 400 eV. The Grimme D2 correction (PBE-D2) was employed and the scaling parameter s_6 in the PBE-D2 scheme was set as 0.6 with the other parameters remained as default values.[2] The validity of the current PBE-D2 setting was well-confirmed in the reproduction of the H_2-benzene interaction energy calculated by the accurate post Hartree-Fock methods, that is, the MP2/aug-ccpVQZ method and the CCSD(T)/complete basis set method.[2] We calculated the total energy of a diatomic molecule and CNT(15,0), $E_{tot}(R, \chi_{CNT})$, by the PBE-D2 scheme as a two dimensional (2D) function of the distance R and the angle $\chi_{CNT} = 0, \pi/12, \pi/6, \pi/4, \pi/3, 5\pi/12$, and $\pi/2$ graphically defined in Fig.S3. The analytical function of the total energy,

$$E_{tot}(R, \chi_{CNT}) = a\left[\left(\frac{b(\chi_{CNT})}{R}\right)^{6.8} - \left(\frac{b(\chi_{CNT})}{R}\right)^{5.5}\right], \tag{1}$$

was obtained by fitting the DFT-calculated total energy data points with the two coefficients a and $b(\chi_{CNT})$. While the coefficient $a = 8255.74$ K was found to be almost independent of χ_{CNT}, the other coefficient $b(\chi_{CNT})$ was obtained as a function of χ_{CNT} (Fig.S3(c)):

$$b(\chi_{CNT}) = 1.558 + \exp\left[-\frac{\cos^2\chi_{CNT}}{10.6}\right] \simeq 2.558 - \frac{\cos^2\chi_{CNT}}{11.1}. \tag{2}$$

The interaction potential energy between the molecule and CNT(15,0), $E_{CNT}(R)$ shown in Fig.S4, was calculated further by symmetrically averaging $E_{tot}(R, \chi_{CNT})$ with respect to

χ_{CNT} to take into account the symmetric interaction of the molecule with CNT(15,0):

$$E_{CNT}(R) = \frac{1}{4\pi}\int_0^{\pi} \sin\chi_{\mathrm{CNT}} d\chi_{CNT} \int_0^{2\pi} d\omega_{CNT} E_{tot}(R, \chi_{\mathrm{CNT}}). \quad (3)$$

The molecule-CNT(15,0) interaction force $\mathbf{F}_{CNT}$ equally acting on two nuclei composing the same molecule was calculated from the gradient of $E_{CNT}(R)/2$, and added to eq.(1).

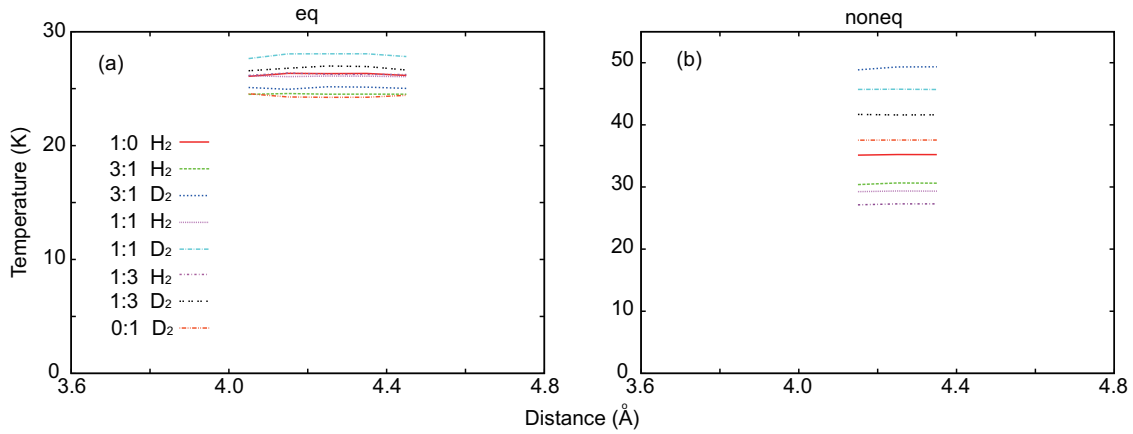

Figure S1: Temperature as a function of the radial distance whose origin is located at the CNT(15,0) center in (a) the equilibrium states at the high temperature and (b) the nonequilibrium states at the high temperature. No data is shown in the region where the molecules can hardly visit during the current 3 ns simulations. In all the cases, the temperature is almost uniform and higher in the nonequilibrium states than in the equilibrium states. The order of the average temperature in the nonequilibrium states is determined by the extent of the flow velocity (Fig.S9(f)) as well as the molecular mass order: On one hand, the faster the nonequilibrium flow is, the higher the average temperature is. On the other hand, the heavier the mixture mass is, the higher the average temperature is. The totally lower temperatures of the H_2 molecules achieved in the nonequilibrium states contribute to the stronger supercooling of the H_2 molecules.

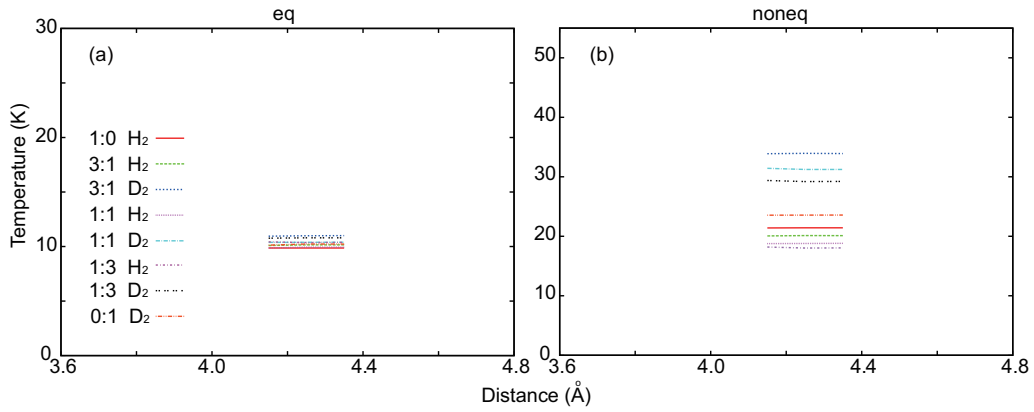

Figure S2: The same as Fig.S1 but at the low temperature. The order of the average temperature in the nonequilibrium states is also determined by the extent of the flow velocity (Fig.S10(f)) as well as the molecular mass order. The totally lower temperatures of the H_2 molecules achieved in the nonequilibrium states contribute to the stronger supercooling of the H_2 molecules.

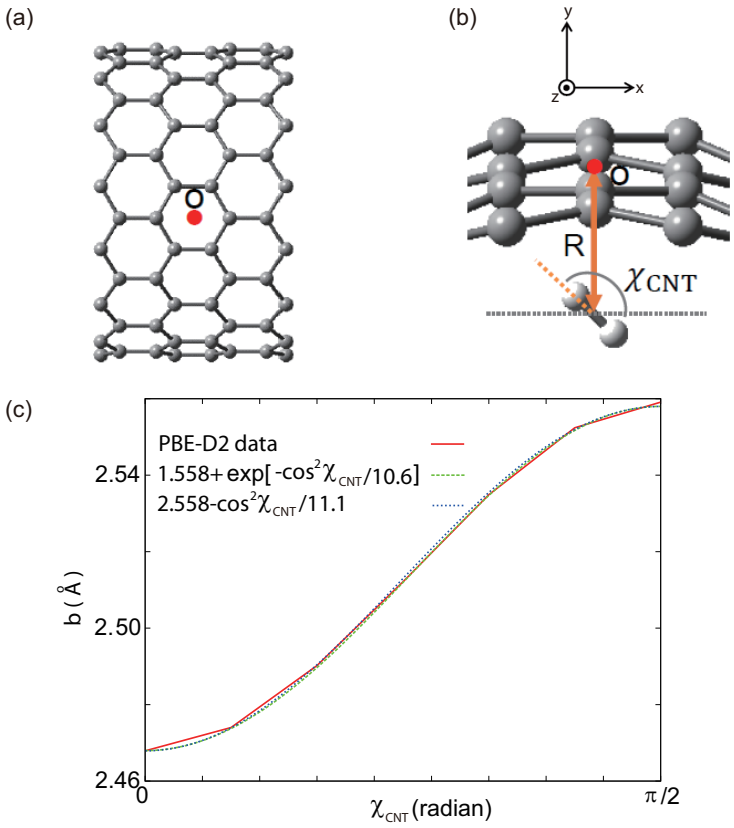

Figure S3: (a) Adsorption site **o** on the CNT(15,0) surface located at the center of a carbon ring of CNT(15,0). (b) Distance R between the center of mass (COM) of a diatomic molecule and the adsorption site **o**. χ_{CNT} is an angle between the molecular axis and the x-axis. (c) Coefficient $b(\chi_{CNT})$ as a function of χ_{CNT}.

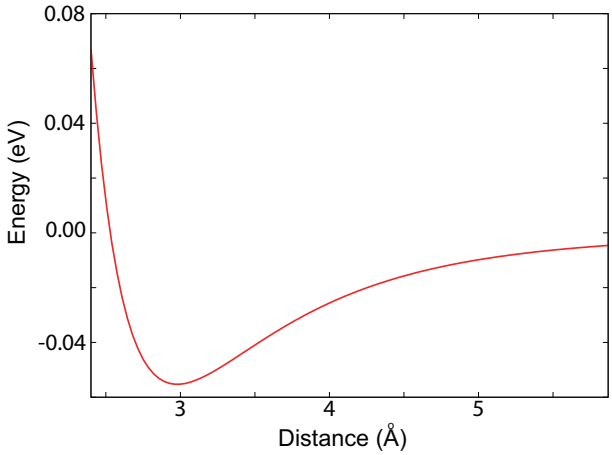

Figure S4: Interaction potential energy between the molecule and CNT(15,0), $E_{CNT}(R)$, as a function of the distance R defined in Fig.S3(b).

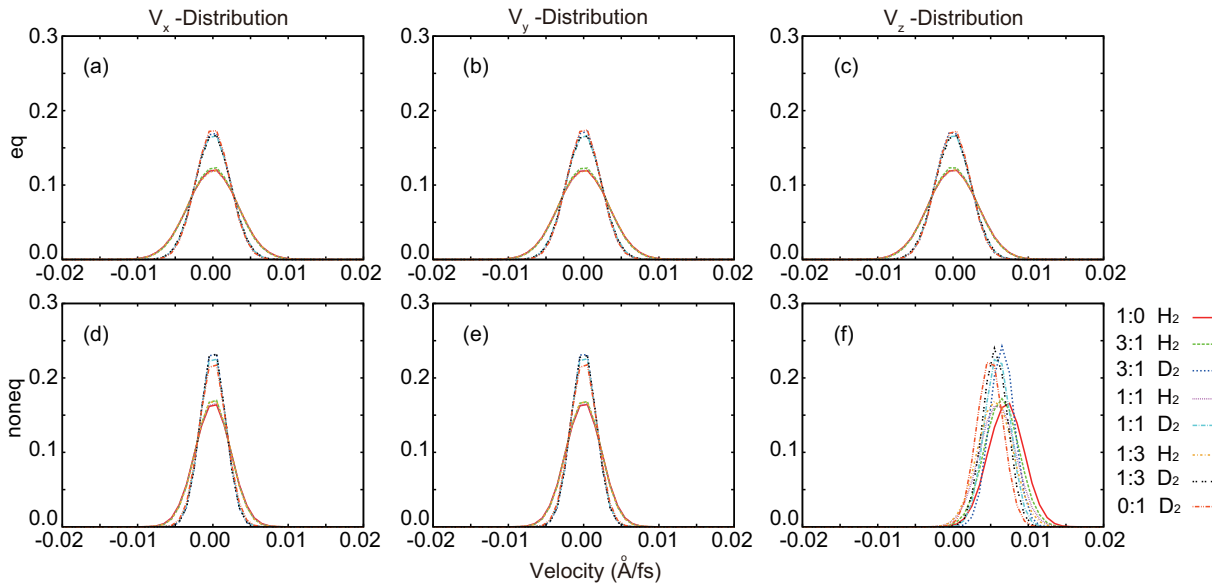

Figure S5: Distributions of the COM velocity V_x, V_y, and V_z at the high temperature (a-c) in the equilibrium states and (d-f) under the nonequilibrium flows. The distributions are broader for the lighter H_2 molecules than for the heavier D_2 molecules. The peak V_z velocity is the same regardless of the isotopes in the same mixture, being in harmony with Figs.S9 and S10. The nonequilibrium flow makes the **V**-distributions sharper due to the flow-induced condensation. The average values of V_x, V_y, and V_z are shown in Fig.S9.

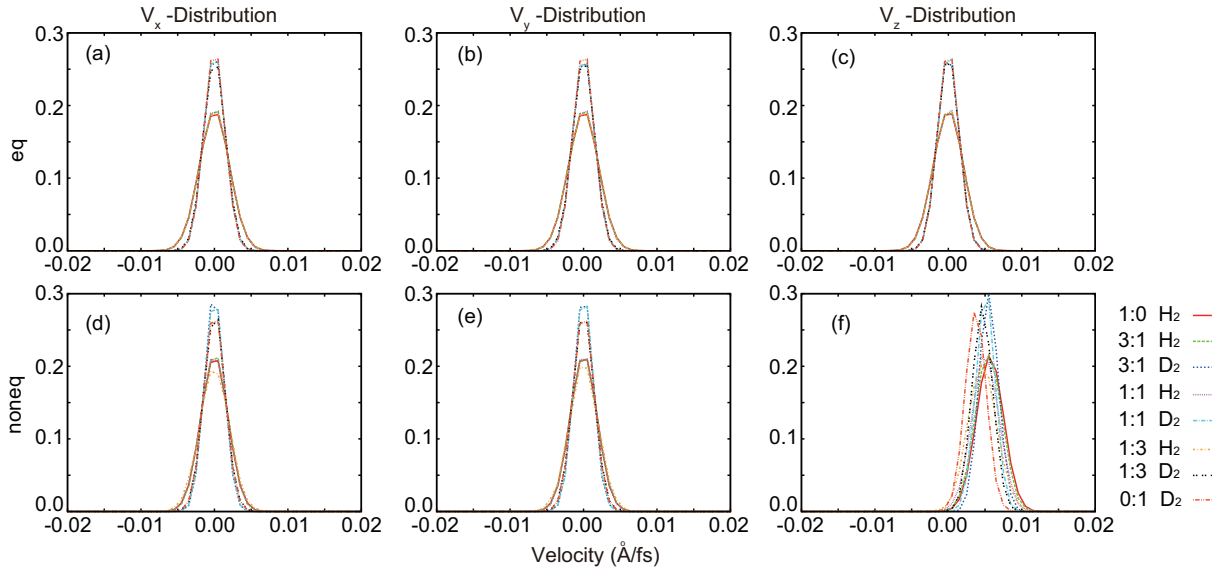

Figure S6: The same as Fig.S5 but at the low temperature. All the distributions become sharper at the low temperature than at the high temperature regardless of the mixing ratios both in the equilibrium and nonequilibrium states. The average values of V_x, V_y, and V_z are shown in Fig.S10.

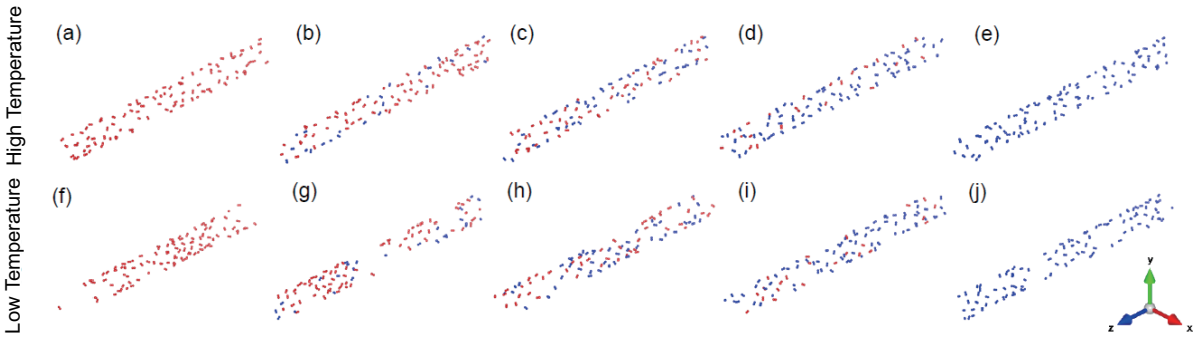

Figure S7: Snapshots of the H_2 (red) and D_2 (blue) molecules at (a-e) the high temperature and (f-j) the low temperature confined inside CNT(15,0) in the equilibrium states. The D_2 ratio increases as (a,f) 0 %, (b,g) 25 %, (c,h) 50 %, (d,i) 75 %, and (e,j) 100 % from the left to the right. The confined 2D mixture films become clearly more structured and non-uniform at the low temperature.

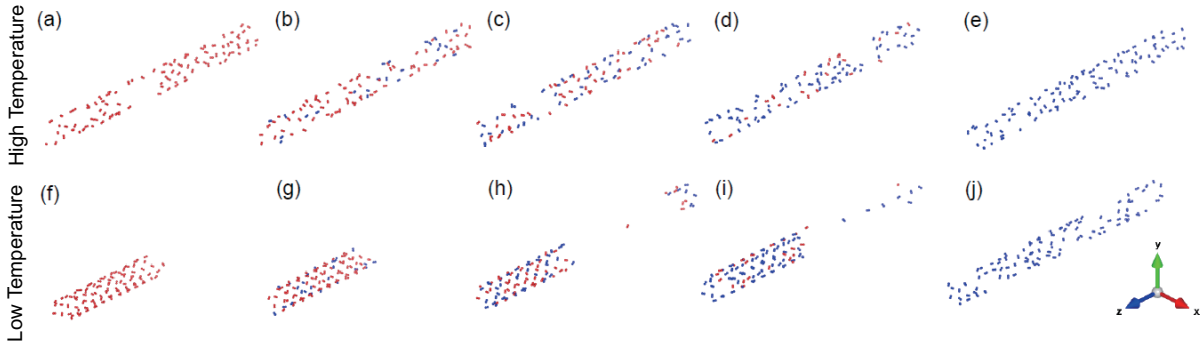

Figure S8: The same as Fig.S7 but under the nonequilibrium flow. In the nonequilibrium state, the structures of the 2D mixture films become non-uniform even at the high temperature.

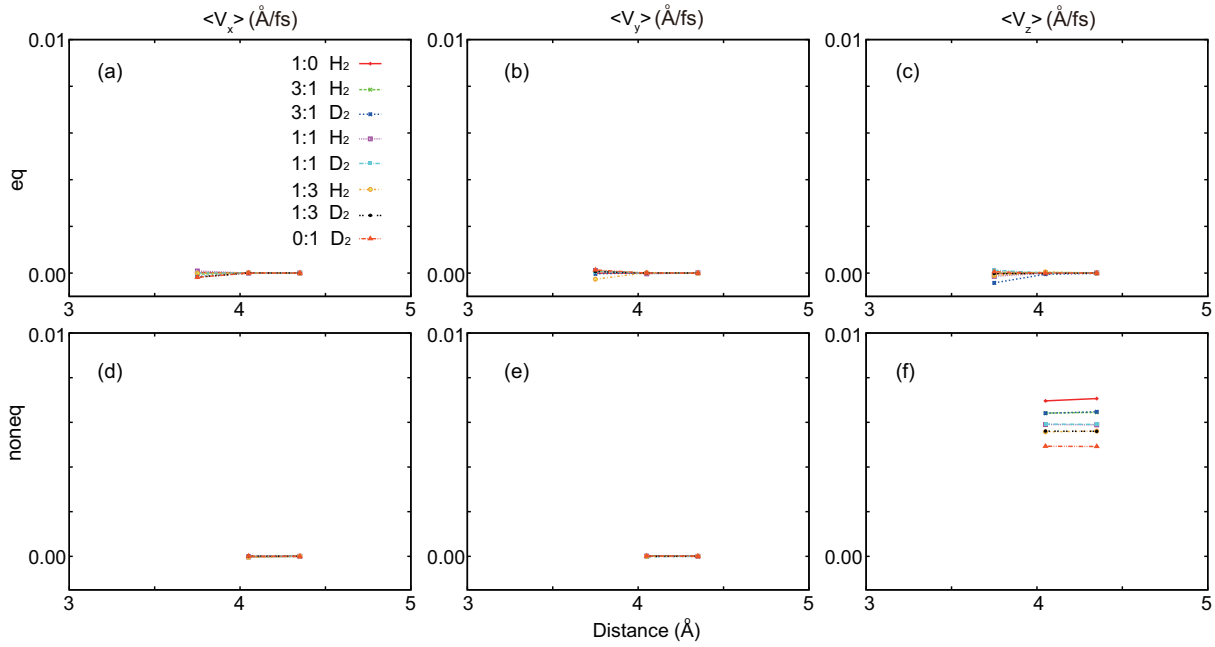

Figure S9: Average velocity as a function of the radial distance from the CNT(15,0) center, $\langle V_x \rangle$, $\langle V_y \rangle$, and $\langle V_z \rangle$ at the high temperature (a-c) in the equilibrium states and (d-f) under the nonequilibrium flows. No data is shown in the region where any molecules can rarely visit during the 3 ns simulations. $\langle V_x \rangle$ and $\langle V_y \rangle$ are almost zero regardless of the mixing ratio both in the equilibrium and nonequilibrium states. $\langle V_z \rangle$ in the equilibrium states is also almost zero. $\langle V_z \rangle$ has a slight gradient along the radial distance under the nonequilibrium flow, meaning that a nonequilibrium shear flow exists inside CNT(15,0). The overall values of $\langle V_z \rangle$ are smaller as the D_2 mixing ratio becomes higher since the heavier liquids are harder to accelerate. Note that $\langle V_z \rangle$ of the H_2 and D_2 molecules are almost identical in the same mixture because of the energy exchange among all the molecules through the intermolecular interaction.

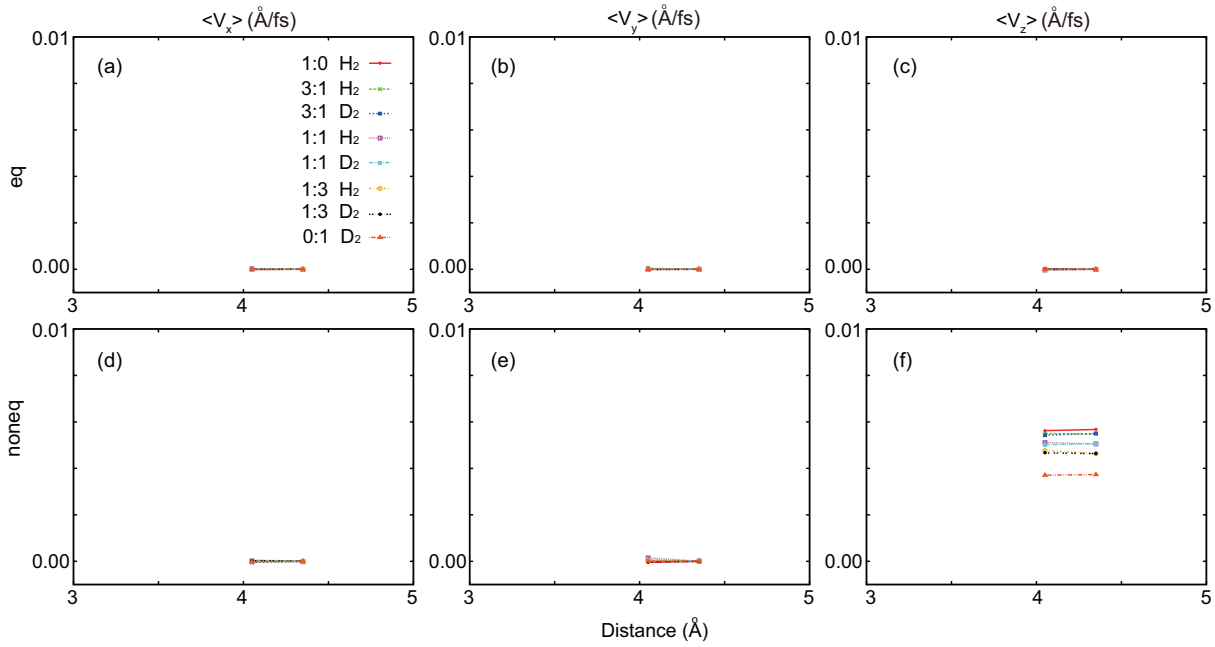

Figure S10: The same as Fig.S9 but at the low temperature.

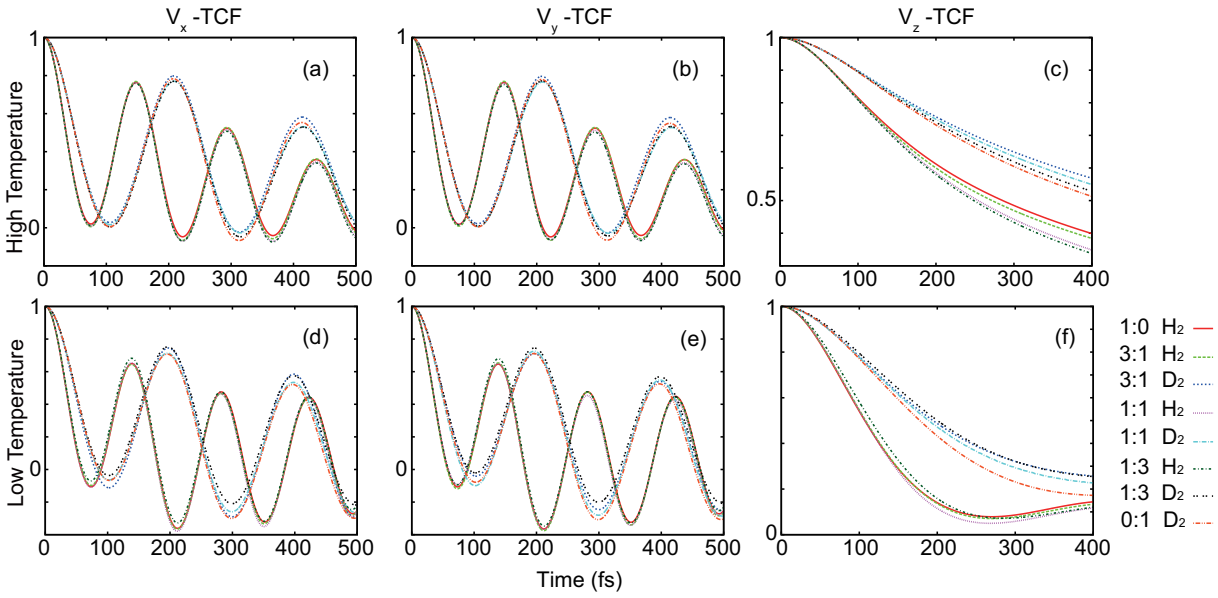

Figure S11: The same as Fig.3 but in the equilibrium states.

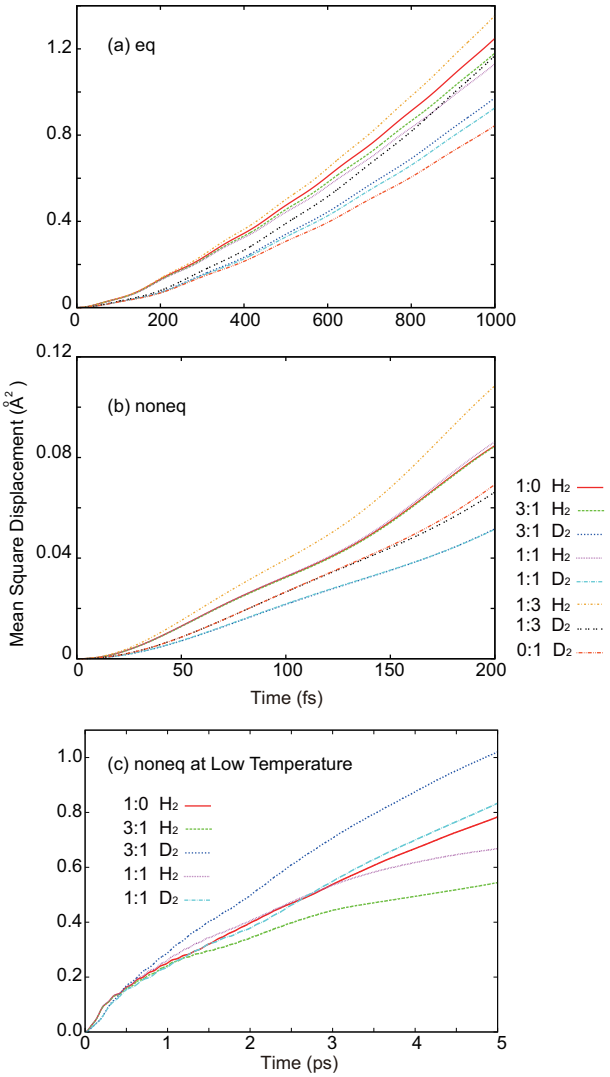

Figure S12: Initial mean-square-displacements at the low temperature in the (a) equilibrium and (b) nonequilibrium states. (c) Magnified Fig.4(d) without the 1:3 and 0:1 mixtures.

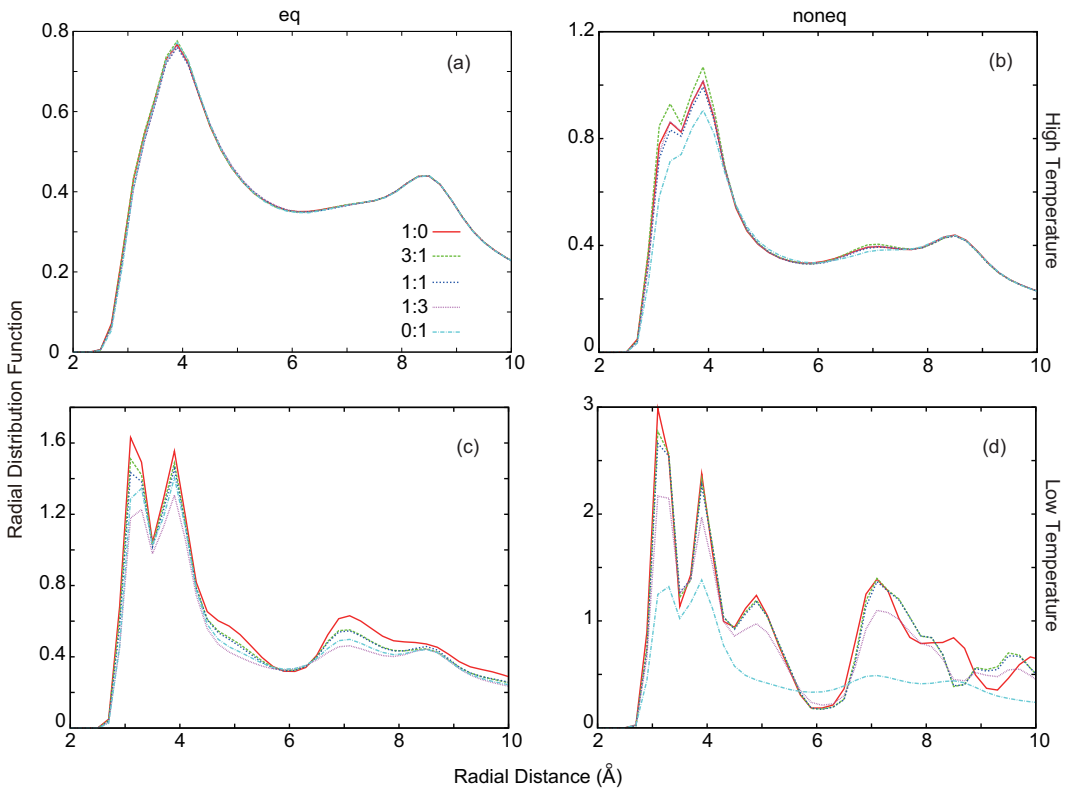

Figure S13: Radial distribution functions (RDFs) at (a) the high temperature in the equilibrium states, (b) the high temperature under the nonequilibrium flows, (c) the low temperature in the equilibrium states, and (d) the low temperature under the nonequilibrium flows. Because the 0:1 mixture exhibits little flow-induced condensation at the low temperature as shown in Fig.1(j), the RDFs are almost similar in the equilibrium and nonequilibrium states, resulting in the smallest RDF of the 0:1 mixture under the nonequilibrium flow.(The light-blue line in Fig.S13(d))

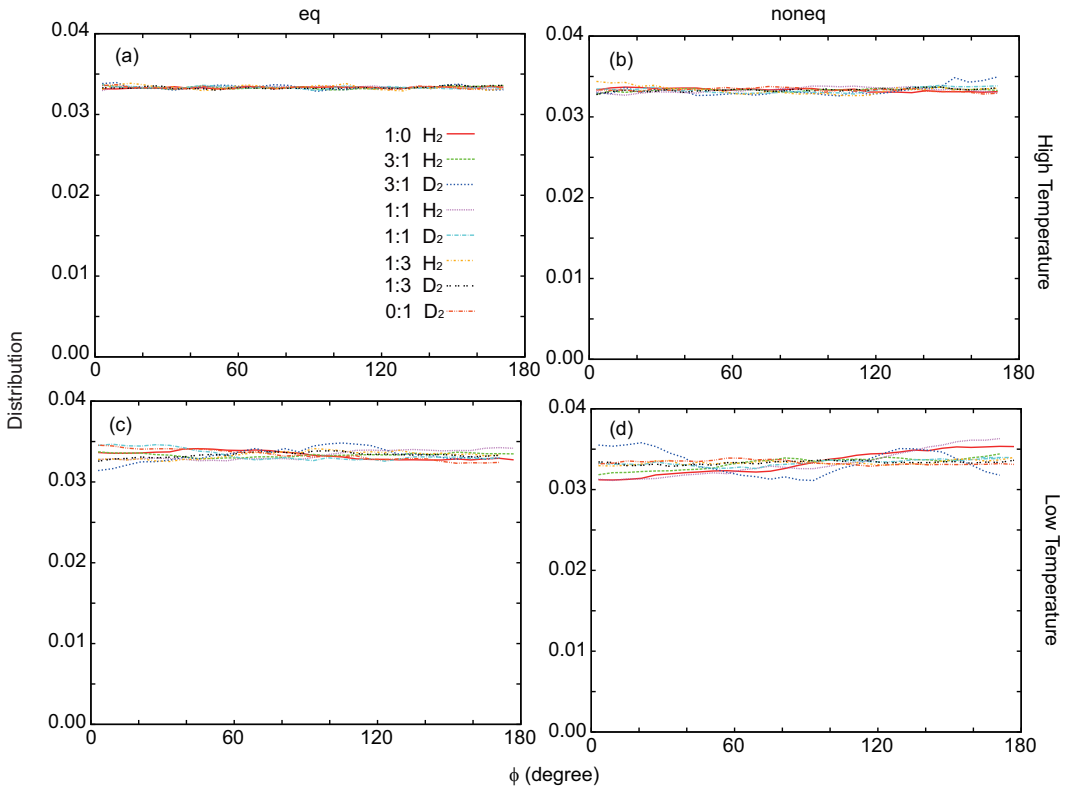

Figure S14: Distributions of the molecular orientation $\phi(t)$ from the z-axis at (a) the high temperature in the equilibrium states, (b) the high temperature under the nonequilibrium flows, (c) the low temperature in the equilibrium states, and (d) the low temperature under the nonequilibrium flows. The ϕ-distributions are almost uniform regardless of the mixing ratio and thermodynamic conditions.

References

(1) Kresse, G.; Furthmüller, J. *Phys. Rev. B* **1996**, *54*, 11169–11186.

(2) Faginas-Lago, N.; Yeni, D.; Huarte, F.; Wang, Y.; Alcami, M.; Martin, F. *J. Phys. Chem. A,* **2016**, *120*, 6451–6458.